ADVANCED MATERIALS

# Tuning the Field Emission Properties of Patterned Carbon Nanotube Films**

By *Jean-Marc Bonard*,* *Nicolas Weiss*, *Hannes Kind*, *Thomas Stöckli*, *László Forró*, *Klaus Kern*, and *André Châtelain*

We demonstrate here the possibility of tuning the field emission properties of carbon nanotube film emitters. Patterned nanotube films were realized by chemical vapor deposition (CVD) combined with soft lithography, which allows one to vary the density of nanotubes on the films. We show that the geometrical arrangement has a determining influence on the field emission properties, and has important consequences for the realization of nanotube field emission devices such as displays. In particular, medium density films with nanotubes protruding over the substrate showed the lowest emission fields and reached current densities of 10 mA cm$^{-2}$ below 4 V/μm. A decrease or increase of the nanotube density resulted in degraded emission properties.

The necessity to display information is central to much of modern science and technology, and displays have nowadays become indispensable. Diverse types of flat panel displays are currently in use but are not always satisfying the requirements of demanding applications. Different solutions are under consideration with major concerns on production costs, long-term stability, and scale up.

Field emission has been recognized early as an attractive alternative to liquid crystal displays (LCDs). In such a device, electrons are extracted from an emitter or emitter array and bombard a phosphor layer deposited on the counter electrode to produce light. Commercial field emission displays based on Mo tips provide a superior picture quality and higher luminosity than LCDs but show high fabrication costs and extreme sensitivity to contamination by adsorbates. Every effort has been made to develop field emitters based on carbon-containing materials (e.g., diamond, diamond-like carbon, and tetrahedral-amorphous carbon) to circumvent those problems. The high expectations and promises held by these materials, however, have not yet been matched by their performances.

Carbon nanotubes (CNTs) have recently emerged as one of the most promising electron field emitters.[1] The power of CNTs as electron sources for displays and lighting devices was amply demonstrated in the last few years. Lighting elements based on CNT cathodes have been presented in 1998 and are commercially available with lifetimes in excess of 8000 h.[2–5] Samsung developed last year a sealed full-color 9″ display.[6,7] CNT cathodes have been incorporated in gas discharge tubes for overvoltage protections[8] and in microwave tubes.[9,10]

The Samsung CNT displays represent an impressive feat and an important milestone towards a fully functional device. They work up to now in diode configuration, which implies that the brightness of a pixel is controlled by varying the potential between emitter and phosphor screen, which is on the order of several kilovolts. Conversely, a triode configuration incorporates a control electrode located near the emitter, and the brightness of the pixel is then controlled by adjusting the potential between cathode and control electrode.

For both diode and triode configuration patterns of CNTs have to be defined on the substrate. This has been demonstrated using different techniques: offset printing,[6,7,11] standard lithography,[12–17] soft lithography,[18–21] and self-assembly.[22–24]

We use here microcontact printing (μCP) to pattern Si substrates with catalyst and subsequently grow CNTs by CVD of acetylene. The advantage of μCP is that the catalyst is applied in liquid form to an elastomeric stamp prior to the transfer to the substrate. Varying the concentration of catalyst in the solution (also called "ink") influences directly the density of CNTs on the patterned film. We demonstrate here that this approach allows one in turn to tune the electron emission properties of the films.

We consider ten patterned (samples A–J) and one continuous (sample K) CNT films obtained with different ink concentrations as summarized in Table 1. Figure 1 displays the effect of ink concentration for five different films and provides an overview of the different samples. Diluted inks (1 mM, sample B) yielded films of low density with very short and thick

Table 1. Emission characteristics of the CNT films studied in this work [a].

| # | ink concentration [mM] | $E_{i,bef}$ [V/μm] | $E_{i,aft}$ [V/μm] | $E_{to}$ [V/μm] | $E_{thr}$ [V/μm] | $\beta_{film}$ | CNT density |
|---|---|---|---|---|---|---|---|
| A | 1 | 6.7 | 12.3 | 16.1 [b] | 21.4 [b] | 255 ± 50 | very low |
| B | 1 | 9.4 | 6.9 | 9.8 | 14.4 | 454 ± 12 | low |
| C | 5 | 2.0 | 3.6 | 5.5 | 7.0 | 851 ± 14 | medium |
| D | 50 | 1.8 | 2.3 | 2.9 | 4.4 | 1363 ± 23 | medium |
| E | 20 | 1.9 | 2.2 | 2.7 | 3.9 | 967 ± 9 | medium |
| F | 50 | 1.0 | 1.8 | 2.2 | 3.3 | 1208 ± 55 | medium |
| G | 40 | 1.2 | 1.9 | 2.3 | 3.5 | 1509 ± 76 | medium |
| H | 40 | 1.2 | 2.5 | 3.2 | 4.9 | 1175 ± 156 | medium |
| I | 50 | 2.1 | 2.9 | 3.6 | 5.3 | 863 ± 62 | high (walls) |
| J | 40 | 3.6 | 3.8 | 5.2 | 7.9 | 712 ± 22 | high (walls) |
| K | 40 | 4.9 | 4.6 | 5.6 | 9.1 [b] | 551 ± 13 | high (continuous film) |

[a] $E_{i,bef}$ and $E_{i,aft}$ are the electric fields needed to extract a current density of 10 nA cm$^{-2}$ before and after the training step. $E_{to}$ and $E_{thr}$ are the turn-on and threshold fields, correspond to current densities of 10 μA cm$^{-2}$ and 10 mA cm$^{-2}$ after training. $\beta_{film}$ is the field amplification factor extracted from the low current *I–V* characteristics after training. [b] The indicated value was extrapolated.

[*] Dr. J.-M. Bonard, N. Weiss, Dr. H. Kind,[+] Dr. T. Stöckli, Dr. L. Forró, Prof. K. Kern,[++] Prof. A. Châtelain
Département de Physique, École Polytechnique
Fédérale de Lausanne, CH-1015 Lausanne EPFL (Switzerland)
E-mail: jean-marc.bonard@epfl.ch

[+] Present address: Department of Chemistry, University of California, Berkeley, CA 94720, USA.

[++] Second address: Max-Planck-Institut für Festkörperforschung, Heisenbergstrasse 1, D-70569 Stuttgart, Germany.

[**] We are grateful to the Centre Interdépartemental de Microscopie Electronique of EPFL (CIME-EPFL) for access to SEM and TEM facilities, as well as to Claude Blanc, Michel Fazan, and André Guisolan (IPE-EPFL) for technical support. The work was partly supported by the Swiss National Science Foundation.

  0935-9648/01/0302-0184 $ 17.50+.50/0 

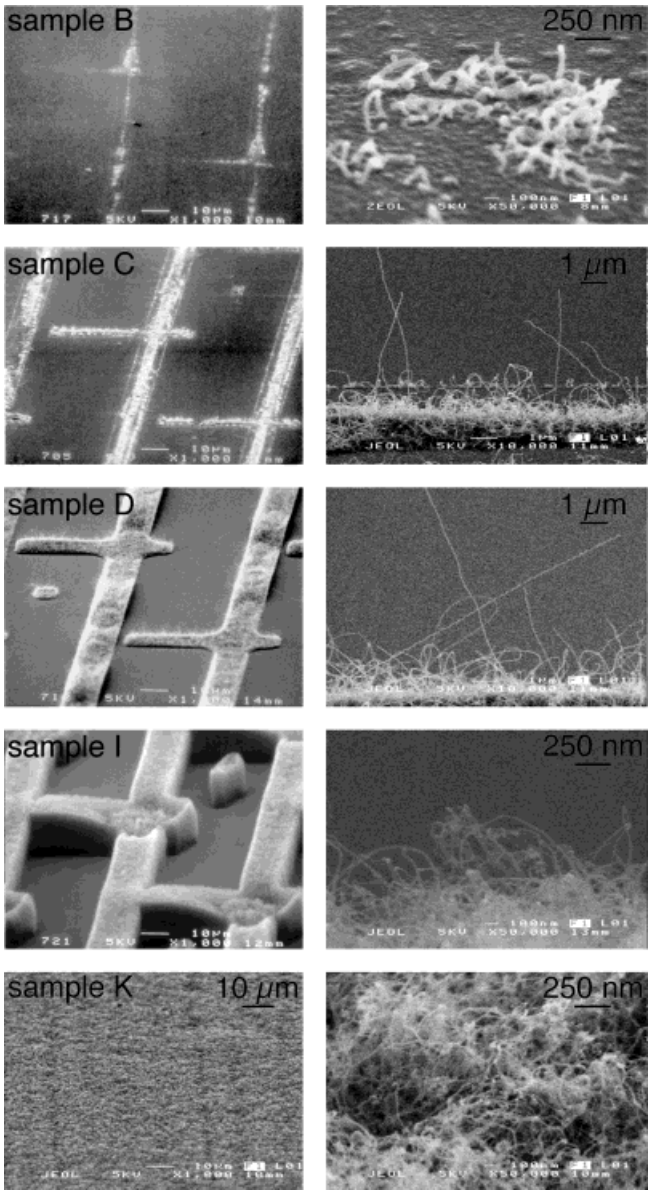


Fig. 1. Low and high magnification SEM micrographs at grazing incidence of 20° to the substrate of samples B, C, D, I, and K (see Table 1).

nanotubes. Increasing the concentration to 5 mM resulted in higher CNT densities with some long tubes (sample C). Further increase of the ink concentration produced films with increasingly denser patterns. Inks of 40 and 50 mM caused the formation of either tangled mats with highly protruding CNTs (sample D) or walls of densely packed CNTs of nearly identical lengths growing perpendicular to the substrate (sample I). The continuous film (sample K) shows a density and arrangement similar to the walls of sample I.

μCP a catalyst offers thus not only the possibility to produce high quality patterned films, but also to vary the density of CNTs within the pattern over a wide range. The samples shown in Figure 1 represent a unique opportunity to study in detail the influence of the film morphology on the field emission properties.

On all 11 samples a stable field emission was measured during the first voltage ramp. We found however that the application of high currents degraded the emission. An example acquired on sample G is shown in Figure 2a. The left curve corresponds to the emission of the pristine film and could be reproduced as long as the field remained below 1.3 V/μm, i.e.,

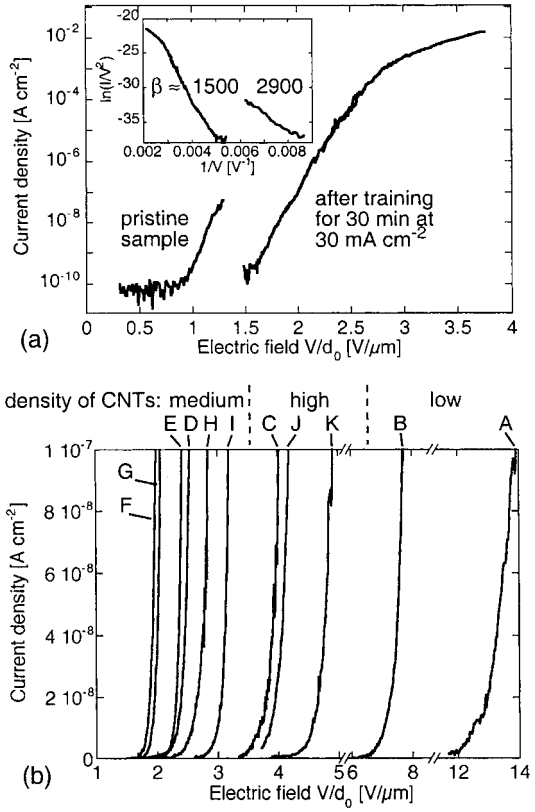


Fig. 2. a) Field emission characteristics of film G (see Table 1) before and after the training step with the corresponding F–N plots in the inset. b) Low current field emission characteristics of the 11 samples after training. The dashed lines are guides for the eye.

the highest field applied so far. It follows a Fowler–Nordheim (F–N) law, i.e., the emitted current $I \propto (F^2/\phi)\exp(B\phi^{3/2}/F)$, with $B = 6.83 \times 10^9$ VeV$^{-3/2}$ m$^{-1}$, $\phi$ the workfunction, and $F$ the local electric field just above the emitter surface.[25] $F$ is usually not known and is often written as $F = \beta E = \beta V/d_0$, where $V$ is the applied voltage, $d_0$ the inter-electrode distance, and $E = V/d_0$ the macroscopic applied field. The field amplification factor $\beta$ is determined solely by the geometrical shape and surroundings of the emitter, and amounts in the case of Figure 2a to $\beta \approx 2900$ (see inset).[25]

The extraction of higher currents resulted invariably in a degradation of the emission that showed up as a shift of the $I$–$V$ curve towards higher fields. This degradation involved also a decrease in the field amplification. We believe that this phenomenon involves some kind of "training" process where the best but mechanically or electrically fragile emitters are damaged or destroyed. To circumvent this problem, we systematically operated the emitters at 30 mA cm$^{-2}$ over a period of 30 min to ensure reproducible characteristics up to 10 mA cm$^{-2}$.

  0935-9648/01/0302-0185 $ 17.50+.50/0 

ADVANCED MATERIALS

In the case of sample G this corresponded to an applied electric field of 4.4 V/μm. Intriguingly, the emitted current remained constant or increased slightly during this training phase.

The *I–V* curve on the right of Figure 2a is the characteristic of sample G after training. The applied field needed for emission has increased by ~60 % and the field amplification has dropped to $\beta \approx 1500$. This behavior was observed on all samples as summarized in Table 1. All the medium and high density samples studied here were capable of emitting at least 10 mA cm$^{-2}$. This value was chosen arbitrarily as the upper limit for our measurements and is not an intrinsic limit of CNTs. In fact, 100 mA cm$^{-2}$ were reached on sample E for a field of 8.2 V/μm, and several groups reported even higher current densities on single- and multi-wall CNT films.[26–28]

We focus now on the influence of the film morphology on the emission properties. Figure 2b shows *I–V* characteristics of the films after the training step at low emitted current densities. Various parameters extracted from the emission measurements are listed in Table 1. The four best films in terms of emission field (samples F, G, E, and D) are of medium density with tubes protruding high out of the CNT mat. They show turn-on and threshold fields below 2.5 and 4.5 V/μm, which puts them among the best CNT field emitters (see Bonard et al.[1] for a recent compilation). Films of lower (sample C) and higher density (samples H, K, and the high density walls of samples I and J) follow at higher fields. All these samples emit consistently below 5 V/μm and have threshold fields below 10 V/μm. The low density films B and A need far higher applied fields. We argue in the following that these differences arise mostly from geometrical and morphological considerations.

Although quite a few studies on field emission from nanotube films have been published since the first reports in 1995, only a few of those compare films of different morphologies. Field emission is a highly selective process and is extremely sensitive to small variations in the chemical nature and shape and/or surroundings of the emitter.[29–32] This makes a comparison of the results obtained by different groups delicate since the growth, purification, film preparation techniques, and the experimental setups differ significantly. The samples studied here consist all of multi-wall CNTs produced by CVD with comparable diameters and offer an ideal opportunity to assess the role of the overall geometry of the emitters.

As noted above, the medium density films are the most efficient emitters, followed by the high and the low density ones. This is pointed out in Figure 3 where the field amplification factor $\beta_{\text{film}}$ is plotted against the onset field after training $E_{\text{i,aft}}$. The samples with the lowest onset fields $E_{\text{i,aft}}$ show also the highest field amplification. Conversely, the low density films required much higher $E_{\text{i,aft}}$. On emitter assemblies like the ones shown in Figure 1, only the CNTs with the highest field amplification will emit, which in turn means that the actual emitter density is lower than the nanotube density by as much as several orders of magnitude.[28,33] To extract some quantitative information from Figure 3, we make the assumptions that the emitter density is identical for all samples, that all CNTs have the same workfunction, and that all CNTs on one given sample have the same field amplification factor. In that case, each emitter has to supply the same current for a given current density regardless of the density and geometrical characteristics of the films. It follows from the F–N model that the local field at the emitter tip, $F_{\text{loc}} = \beta V/d_0$, has to be the same for every emitting tube.[25] One obtains in the case of Figure 3 that $\beta_{\text{film}} = F_{\text{loc}}/(V/d_0) = F_{\text{loc}}/E_{\text{i,aft}}$, i.e., the field amplification varies as the inverse of the onset field with the

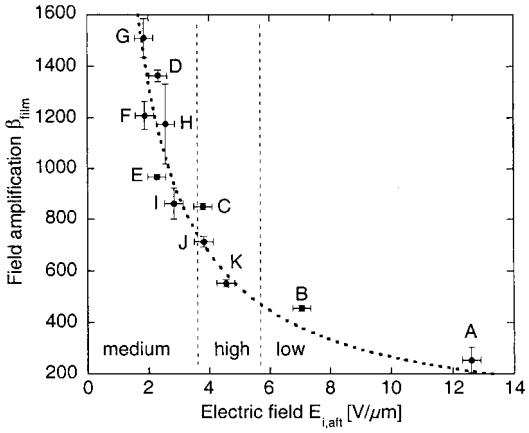


Fig. 3. Field amplification factor $\beta_{\text{film}}$ as a function of the onset field after training, $E_{\text{i,aft}}$. The dotted curve represents the best fit to the formula $\beta_{\text{film}} = F_{\text{loc}}/E_{\text{i,aft}}$ with $F_{\text{loc}} = 2.6 \pm 0.1$ kV/μm.

local field at the emitter surface as the sole parameter. We have fitted the experimental points in Figure 3 with this formula and obtained a local field at the emitter tip of 2.6 ± 0.1 kV/μm. This is quite remarkable, because this value obtained from measurements on 11 different samples corresponds well to the field needed to initiate field emission on one emitter. It has to be noted that this result does not validate the above assumptions. In particular, the emitter density varies probably significantly from sample to sample, but its influence is minimized by the highly nonlinear increase of emitted current with the applied field: a variation of emitted current of an order of magnitude coincides with a change of 7 % only in the applied field as can be extracted from Figure 2.

It is therefore not surprising that not all experimental points in Figure 3 fall on the fitted curve. If two samples show the same field amplification, as I (high density walls) and C (low to medium density), the film with the higher onset field (C) should also have the lower emitter density. This is confirmed by scanning electron microscopy (SEM) observations. Conversely, if two samples have similar onset fields, as J and C for example, the film with the higher field amplification (C in that case) should have a lower emitter density. This fact is less obvious to extract from the SEM micrographs and warrants some more attention.

Which parameters determine the field amplification? A simple electrostatic model suggests that $\beta_{\text{tube}}$ for a single tube can be described as $\beta_{\text{tube}} \propto h/r$, where $h$ is the height and $r$ the radius of the emitter. The influence of the height is significant

  0935-9648/01/0302-0186 $ 17.50+.50/0 

even for several micrometer long tubes as proven by electrostatic calculations. Another effect manifests itself as soon as several emitters are assembled to form a multiple source: screening between the emitters become significant even for large inter-tube distances. Figure 4a reveals the dependance of the field amplification factor ($\beta_{film}$) on the intertube distance $l$ as estimated from electrostatic calculations.[34,35] For clarity $\beta_{film}$ is normalized by the field amplification $\beta_{tube}$ for a single tube. The field amplification drops rapidly for inter-tube distances $l \leq 2h_0$. Since the density of emitters increases with decreasing distance, there is an optimum distance for a maximal emitted current density that amounts to 1–2 times the tube height.[34,35]

We try in the following to estimate $\beta_{film}$ by taking the morphology of the films into account. The electrostatic calculations reported in the literature[34,35] were performed for a given height $h_0$ of 2 μm. It appears that variations of the radius of curvature $r$ or the inter-electrode distance $d_0$ change the absolute value of $\beta_{film}$, but that the dependence on the inter-tube distance is not affected. We extract from the calculations a function $f(l) = 1 - \exp(-1.1586l)$ reproduced in Figure 4a that characterizes the decrease in field amplification due to inter-tube screening. To determine $f(l)$ for $h \neq h_0$, $l$ has simply to be scaled by $h_0/h$ since $f(l)$ does not depend on $r$ and $d_0$. By taking $\beta_{tube} \propto h/r$, we can write $\beta_{film}(l,h,r) = \beta_{tube}f(lh_0/h) \propto (h/r)f(lh_0/h)$. We then estimate the field amplification for our samples from the parameters $h$, $r$, and $l$ obtained from the SEM observations and summarized in Table 2.

Table 2. Morphological characteristics of the CNT films as estimated from SEM observations [a].

| # | $\rho$ [μm$^{-2}$] | $r$ [nm] | $h$ [μm] | $l$ [μm] |
|---|---|---|---|---|
| A | 0.1 | 25±3 | <0.18 | 1.8±0.5 |
| B | 1 | 18±3 | 0.4±0.2 | 0.5±0.2 |
| C | 60 | 19±3 | 3.01±1.5 | 1.02±0.5 |
| D | 110 | 21±3 | 2.93±1.9 | 2.0±1.0 |
| E | 100 | 18±3 | 2.56±1.2 | 2.05±0.7 |
| F | 75 | 19±3 | 3.46±1.1 | 1.89±1.0 |
| G | 45 | 13±3 | 2.29±0.7 | 1.46±0.5 |
| H | 150 | 11±2 | 1.53±0.8 | 2.9±1.4 |
| I | 500 | 11±2 | 0.96±0.48 | 0.81±0.16 |
| J | 340 | 10±2 | 0.78±0.35 | 1.51±0.35 |
| K | 280 | 10±2 | 0.5±0.3 | 0.6±0.2 |

The surface density $\rho$ refers to the total tube density. The mean height $h$ over the CNT mat or substrate and the inter-tube distance $l$ characterize the potential field emitters, i.e., the nanotubes protruding out of the film. $r$ is the mean tube radius.

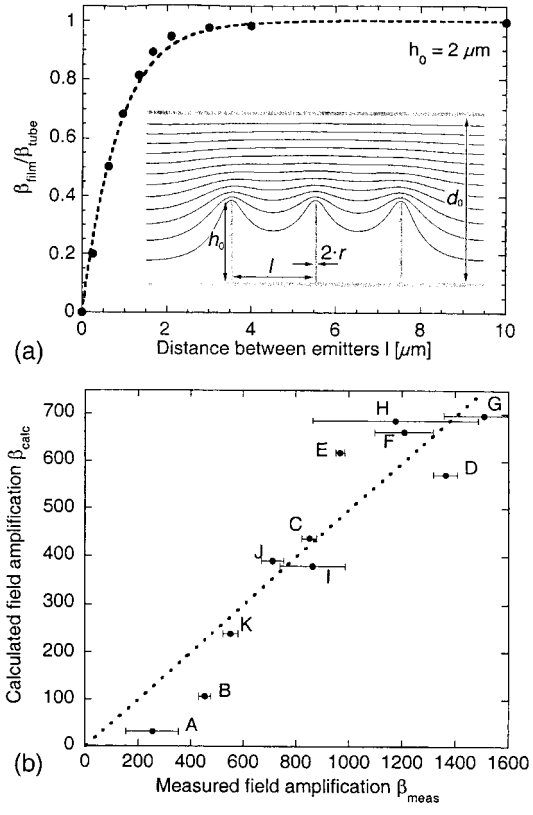


Fig. 4. a) Field amplification $\beta_{film}/\beta_{tube}$ as a function of the inter-tube distance $l$ for a nominal height $h_0 = 2$ μm. The dashed line corresponds to the function $f(l) = 1 - \exp(-1.1586l)$ obtained by fitting from the simulated values. The inset shows a typical electrostatic simulation of the equipotentials around an array of emitters. b) Measured ($\beta_{meas}$) versus calculated ($\beta_{calc}$) field amplification factor. The dotted line is a simple proportional regression $\beta_{calc} \propto \beta_{meas}$. Error bars for the experimental values correspond to the statistical standard deviation. The error in $\beta_{calc}$ arising from the spread of $l$, $r$, and $h$ (see Table 2) is typically ±30 %.

We display in Figure 4b the measured versus the calculated field amplification. The dotted line is a simple proportional regression. Our simple estimate does not yield an absolute value for the field amplification, but it allows us to reproduce the experimental tendency with a reasonable accuracy. We note also that the field amplification for the low density films are underestimated. We have to recall that field emission is highly selective and that only the tubes with the highest field amplification factor will show a significant emission. The SEM observations used for the determination of $l$, $h$, and $r$ encompassed an area of ~$2 \times 10^{-6}$ cm$^2$. This has to be compared with a typical emitter density of $10^4$ cm$^{-2}$ at the very beginning of emission,[28,33] i.e., one emitter per $10^{-4}$ cm$^2$. The probability of including a representative environment of the emitting tubes in the SEM statistics is thus very small for the low density films, which are far less homogenous than the medium- and high-density films.

It appears from the above discussion that geometrical considerations determine to a great extend the field emission properties of CNT films. The height and inter-tube distance have a determining influence on the emitted current density, and films with very high densities of CNTs are not necessarily optimal field emitters.

These considerations can be extended and confirmed by characterizing the emission on a microscopic scale, as opposed to the integral measurements presented here. This has been done by Nilsson et al. on similar samples prepared by the same method.[34] The local field emission properties were measured in a vacuum field emission apparatus by scanning a

  0935-9648/01/0302-0187 $ 17.50+.50/0 

ADVANCED MATERIALS

sharp anode over the film. Such a technique is an enticing alternative to the integral characterization since microscopic measurements sample all potential field emitters, whereas integral field emission is far more selective as only the most prominent emitters contribute to the emitted current. Nilsson et al. observed a rather inhomogeneous emission pattern on low density films. The emission was far more homogenous for medium density films as all the features of the patterns could be clearly detected. High density films yielded results comparable to the low density ones but with an emitted current higher by one order of magnitude.

What does the ideal film field emitter look like? Our study answers at least part of the question. We have noted that the emission fields for low density films are high because there are few emitters with small heights. Conversely, the emission from high density films is more efficient but remains low because of screening effects between densely packed neighboring tubes and because of the small height of the few protruding tubes. There is an ideal compromise between these two extremes, where the height of the tubes ($h \approx 3$ μm) and the distance between neighboring emitters ($l \approx 2$ μm) are both sufficient to reach a high field amplification along with an emitter density that is high enough to ensure homogeneous emission at low fields. In that light, μCP is an attractive method to produce patterned CNT films by CVD as it allows to tune the density of nanotubes in the patterns, and hence to optimize the field emission properties of the film.

## *Experimental*

*Growth of Patterned CNT Films*: The detailed stamp and catalyst preparation procedures have been described in detail elsewhere [18,21]. Our catalyst of choice is an ethanolic solution of 1–50 mM $Fe(NO_3)_3{\cdot}9H_2O$ that has been aged for at least 12 h. Freshly inked stamps were printed on the native oxide of $SiO_2$/Si wafers. The growth of nanotubes was carried out in a horizontal flow reactor at 720 °C working at atmospheric pressure. The system was purged before and after the growth with $N_2$ for 15 min. The actual growth occurred in a mixture of 15 mL/min $C_2H_2$ and 1000 mL/min $N_2$ over a period of 30 min. Transmission electron microscopy (TEM) reveals that the deposition process is highly selective, as the CVD growth produces almost exclusively CNTs with only few catalyst particles [18,21]. The tube walls are well graphitized with graphene sheets running approximately parallel to the tube axis, and most tubes have open ends. Some defects are detected on the tube walls, which is typical of CNTs grown by CVD techniques [36,37].

*Characterization and Field Emission*: The films were systematically characterized by SEM with a Jeol 6300-F operated at 5 kV. The field emission experiments were performed in a ultra high vacuum (UHV) chamber with a base pressure of $10^{-7}$ mbar. The counter electrode was a highly polished stainless steel sphere of 1 cm diameter, leading to an emission area of ~0.007 $cm^{-2}$ according to electrostatic calculations. The emission current was measured with a Keithley 6517A electrometer capable of sourcing up to 1000 V and 1 mA. The patterned substrates were mounted on a linear manipulator and the interelectrode distance $d_0$ was fixed at 125 μm. This distance was halved on the two samples where emission could not be observed below 1000 V.

Received: July 14, 2000
Final version: September 25, 2000

[1] J.-M. Bonard, H. Kind, T. Stöckli, L.-O. Nilsson, *Solid-State Electron.*, in press.
[2] Y. Saito, S. Uemura, K. Hamaguchi, *Jpn. J. Appl. Phys.* **1998**, *37*, L346.
[3] Y. Saito, K. Hamaguchi, S. Uemura, K. Uchida, Y. Tasaka, F. Ikazaki, M. Yumura, A. Kasuya, Y. Nishina, *Appl. Phys. A* **1998**, *67*, 95.
[4] Y. Saito, S. Uemura, *Carbon* **2000**, *38*, 169.
[5] H. Murakami, M. Hirakawa, C. Tanaka, H. Yamakawa, *Appl. Phys. Lett.* **2000**, *76*, 1776.
[6] W. B. Choi, D. S. Chung, J. H. Kang, H. Y. Kim, Y. W. Jin, I. T. Han, Y. H. Lee, J. E. Jung, N. S. Lee, G. S. Park, J. M. Kim, *Appl. Phys. Lett.* **1999**, *75*, 3129.
[7] J. M. Kim, N. S. Lee, W. B. Choi, J. E. Jung, I. T. Han, D. S. Jung, S. H. Park, S. S. Hong, H. Y. Kim, presented at the *14th Int. Winterschool on Electronic Properties of Novel Materials (IWEPNM2000)*, Kirchberg, Austria, March 4–11, **2000**.
[8] R. Rosen, W. Simendinger, C. Debbault, H. Shimoda, L. Fleming, B. Stoner, O. Zhou, *Appl. Phys. Lett.* **2000**, *76*, 1663.
[9] O. Zhou, presented at the *14th Int. Winterschool on Electronic Properties of Novel Materials (IWEPNM2000)*, Kirchberg, Austria, March 4–11, **2000**.
[10] O. Zhou's group (UNC Chapel Hill), W. Zhu (Lucent Technologies), pending US Patents.
[11] Q. H. Wang, A. A. Setlur, J. M. Lauerhaas, J. Y. Dai, E. W. Seelig, R. P. H. Chang, *Appl. Phys. Lett.* **1998**, *72*, 2912.
[12] J. Kong, A. M. Cassell, H. Dai, *Chem. Phys. Lett.* **1998**, *292*, 567.
[13] X. Xu, G. R. Brandes, *Appl. Phys. Lett.* **1999**, *74*, 2549.
[14] Z. F. Ren, Z. P. Huang, D. Z. Wang, J. G. Wen, J. W. Xu, J. H. Wang, L. E. Calvet, J. Chen, J. F. Klemic, M. A. Reed, *Appl. Phys. Lett.* **1999**, *75*, 1086.
[15] S. Fan, M. G. Chapline, N. R. Franklin, T. W. Tombler, A. M. Cassell, H. Dai, *Science* **1999**, *283*, 512.
[16] Y. Yang, S. Huang, H. He, A. W. H. Mau, L. Dai, *J. Am. Chem. Soc.* **1999**, *121*, 10 832.
[17] S. Huang, L. Dai, A. W. H. Mau, *J. Phys. Chem. B* **1999**, *103*, 4223.
[18] H. Kind, J.-M. Bonard, C. Emmenegger, L.-O. Nilsson, K. Hernadi, E. Maillard-Schaller, L. Schlapbach, L. Forró, K. Kern, *Adv. Mater.* **1999**, *11*, 1285.
[19] A. M. Cassell, N. R. Franklin, T. W. Tombler, E. M. Chan, J. Han, H. Dai, *J. Am. Chem. Soc.* **1999**, *121*, 7975.
[20] S. Huang, A. W. H. Mau, T. W. Turney, P. A. White, L. Dai, *J. Phys. Chem. B* **2000**, *104*, 2193.
[21] H. Kind, J.-M. Bonard, L. Forró, K. Kern, K. Hernadi, L.-O. Nilsson, L. Schlapbach, *Langmuir* **2000**, *16*, 6877.
[22] M. Burghard, G. Duesberg, G. Philipp, J. Muster, S. Roth, *Adv. Mater.* **1998**, *10*, 584.
[23] M. Ahlskog, E. Seynaeve, R. J. M. Vullers, C. Van Haesendonck, *J. Appl. Phys.* **1999**, *85*, 8432.
[24] J. Liu, M. J. Casavant, M. Cox, D. A. Walters, P. Boul, L. Wei, A. J. Rimberg, K. A. Smith, D. T. Colbert, R. E. Smalley, *Chem. Phys. Lett.* **1999**, *303*, 1.
[25] See, e.g., J. W. Gadzuk, E. W. Plummer, *Rev. Mod. Phys.* **1973**, *45*, 487. A workfunction of 5 eV was taken for the determination of $\beta$.
[26] L. A. Chernozatonskii, Y. V. Gulyaev, Z. Y. Kosakovskaya, N. I. Sinitsyn, G. V. Torgashov, F. Zakharchenko Yu, E. A. Fedorov, V. P. Val'chuk, *Chem. Phys. Lett.* **1995**, *233*, 63.
[27] P. G. Collins, A. Zettl, *Appl. Phys. Lett.* **1996**, *69*, 1969.
[28] W. Zhu, C. Bower, O. Zhou, G. Kochanski, S. Jin, *Appl. Phys. Lett.* **1999**, *75*, 873.
[29] J.-M. Bonard, J.-P. Salvetat, T. Stöckli, L. Forró, A. Châtelain, *Appl. Phys. A* **1999**, *69*, 245.
[30] Q. H. Wang, T. D. Corrigan, J. Y. Dai, R. P. H. Chang, A. R. Krauss, *Appl. Phys. Lett.* **1997**, *70*, 3308.
[31] D. N. Davydov, P. A. Sattari, D. AlMawlawi, A. Osika, T. L. Haslett, M. Moskovits, *J. Appl. Phys.* **1999**, *86*, 3983.
[32] C. Bower, O. Zhou, W. Zhu, A. G. Ramirez, G. P. Kochanski, S. Jin, *Mater. Res. Soc. Symp. Proc.*, in press.
[33] O. M. Küttel, O. Gröning, C. Emmenegger, L. Nilsson, E. Maillard, L. Diederich, L. Schlapbach, *Carbon* **1999**, *37*, 745.
[34] L. Nilsson, O. Gröning, C. Emmenegger, O. Küttel, E. Schaller, L. Schlapbach, H. Kind, J.-M. Bonard, K. Kern, *Appl. Phys. Lett.* **2000**, *76*, 4079.
[35] O. Gröning, O. M. Küttel, P. Gröning, L. Schlapbach, *J. Vac. Sci. Technol. B* **2000**, *18*, 665.
[36] V. Ivanov, J. B. Nagy, P. Lambin, A. Lucas, X. B. Zhang, X. F. Zhang, D. Bernaerts, G. Van Tendeloo, S. Amelinckx, J. Van Landuyt, *Chem. Phys. Lett.* **1994**, *223*, 329.
[37] A. Fonseca, K. Hernadi, P. Piedigrosso, J. F. Colomer, K. Mukhopadhyay, R. Doome, S. Lazarescu, L. P. Biro, P. Lambin, P. A. Thiry, D. Bernaerts, J. B. Nagy, *Appl. Phys. A* **1998**, *67*, 11.

  0935-9648/01/0302-0188 $ 17.50+.50/0 